CrystEngComm

Accepted Manuscript

ROYAL SOCIETY OF CHEMISTRY

www.rsc.org/crystengcomm

Controlling the Energy Transfer in Lanthanide-Organic Frameworks for White-Light Emitting Materials Production

Leonis L. da Luz [a], Bárbara F. Lucena Viana [b], Gabriel C. Oliveira da Silva [b], Cláudia C. Gatto [b], Adriana M. Fontes[c], Marcos Malta[c], Ingrid T. Weber [b], Marcelo O. Rodrigues [b]* and Severino A. Júnior

[a] *Departamento de Química Fundamental, UFPE, 50670-901, Recife, PE, Brazil. Tel. +55 81 2126-7475; Fax: +55 81 2126-8442;*
[b] *Instituto de Química, Universidade de Brasília, 70910-900, Brasília – DF, Brazil. Tel. +55 61 3107-3876; Fax: +55 61 3273-4149;*
[c] *Instituto de Química, Universidade Federal da Bahia, Campus Ondina, Salvador (BA), Brazil. Fax: 55 71 3237 4117; Tel: 55 71 3283 6850;*

Keywords. lanthanides, luminescence, metal-organic framework, energy transfer.

Abstract. Visible color tunable and white-light emitting Ln-MOFs were obtained via layer-by-layer epitaxial growth of the different $[Ln_2(Mell)(H_2O)_8]$ compounds. The *RGB-MOF*, *RBG-MOF*, *BRG-MOF* and *BGR-MOF* materials exhibits white-light emission, CIE coordinate (0.337, 0.336), (0.339, 0.330), (0.338, 0.337) and (0.333, 0.336), upon excitation at 361, 347, 378 and 360 nm, respectively, very close to standardized value (0.33, 0.33).

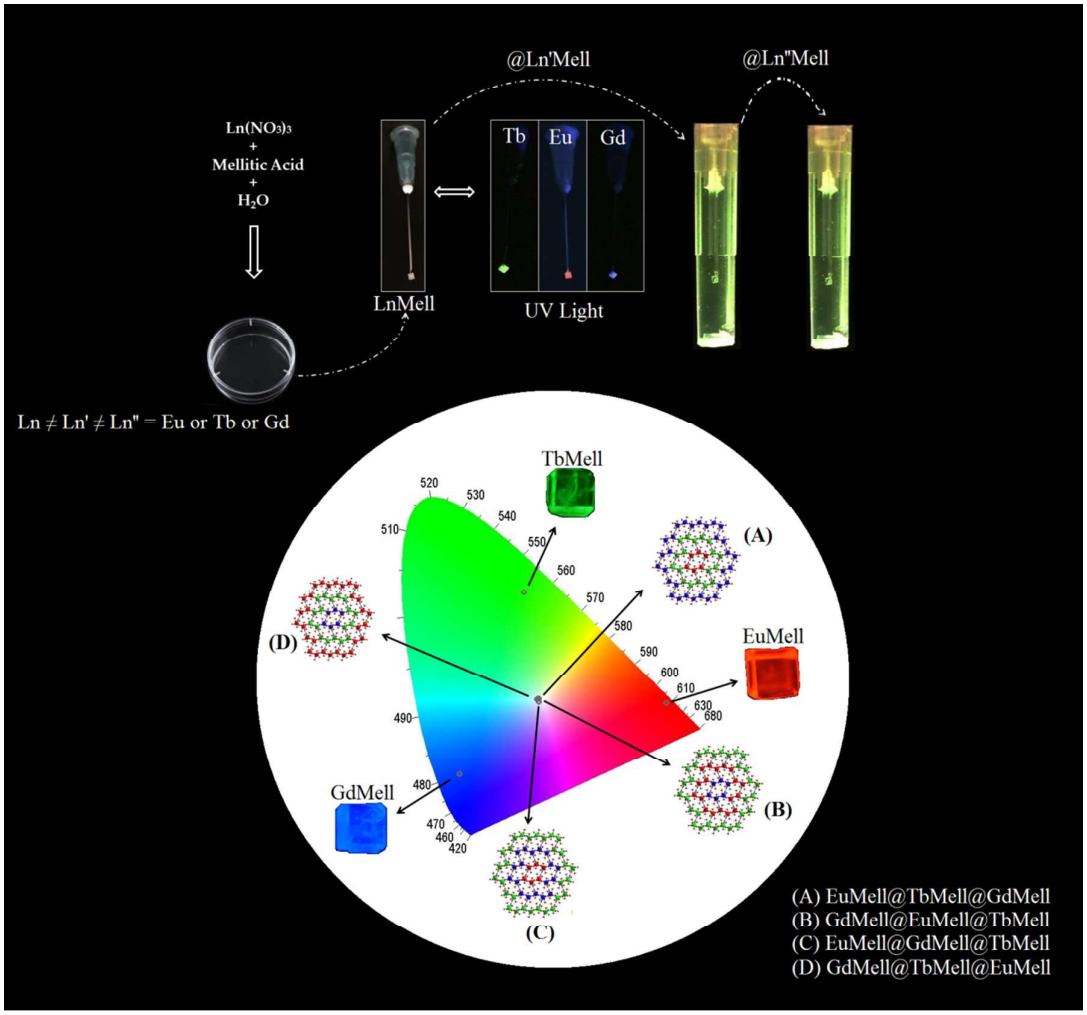

INTRODUCTION

The development of solid state light emitting materials has attracted intense interest to both scientific and industrial communities due to their potential application in areas such as full-colour flat-panel electroluminescent displays for mobile devices, lighting, optical-telecommunications and backlight for liquid-crystal displays.[1, 2] In the vast majority of the reports describe the use of inorganic oxides, polymers, organic molecules or quantum dots for production these devices.[3-5] Recently, however, Metal-Organic Frameworks (MOF) have emerged as a class of organic-inorganic hybrid compounds very interesting for exploration as emissive materials.[6] MOFs present a high degree of structural predictability, chemical and physical robustness, and a well-defined chemical environment for emitter centers.[7] Indeed, the hybrid character of MOFs, including both metal centers or metallic clusters and organic ligands, allows them to produce and a diversity of optical phenomenon uncommon in classical light emitting materials.[8, 9]

Among hundreds of luminescent MOFs reported, indubitably, Lanthanide-Organic Frameworks (Ln-MOFs) are the most promising due to the well-known spectroscopic properties.[10] These photophysical features have been explored in materials science, in particular, in the development of sensors and optical probes in forensic investigation and temperature measurements.[11-15] The design of visible color tunable and white-light emitting Ln-MOFs is still a challenge, because embodies the understanding of each one of the stages involved in energy transfer process in these materials. Indeed, the production of a single component white-light emitter material has been considered as hot-topic of research.[16-18] Currently, the production of color tunable and white light emission with the use of Ln-MOF source consists, basically, in a systematic control of the amount of Eu^{3+} and Tb^{3+} dopants in a blue emitter hybrid matrix.[19] In this case the Ln-MOFs matrix may be composed by optically inactive Ln^{3+} ions such as La^{3+} and an organic linker that emits blue light or based in a blue emitter Ln^{3+} ion.[19-21] In another example, Zhang *et al*. have produced a white light emitter

MOF based on samarium ion. [18] Although these methods have presented interesting results, the distribution of distinct populations of Ln^{3+} ions in the Ln-MOF matrix is fully randomised. Consequently, the independet emissions of each primary color would be quenched due to the energy transfer (ET) among the emitter centers, as observed in several reports in literature.[22] This question may be minimized constraining the emitter centers in specific regions of the crystal domain, through of a sophisticated engineering of high ordered heterostructures. In these materials the interactions among distinct emitter are considerably reduced.

Epitaxial growth of MOF on the surface of another one may be an interesting alternative for production of multicolour emitter materials, nevertheless, this approach has been applied only for complexes and MOF based on transition metals.[23-26] The engineering of the multiemitter-layered MOFs permits the construction White-light-emitting Materials, because enables the best control of the ET processes, mitigating them to the single-crystal interfaces. Therefore, each MOF layer can act as independent crystal, maintaining intact its optical properties. Hence, we wish to present the first example of the use of distinct layer-by-layer epitaxial growing of Ln-MOFs ($[Ln_2(Mell)(H_2O)_8]$ materials— Mell = Mellitate anion and Ln = Eu^{3+}, Tb^{3+} and Gd^{3+}, hereafter *R-MOF*, *G-MOF* and *B-MOF* for production of visible color tunable and white-light emitting materials. The experimental procedure described by Munkata *et al.*[27] for synthesis of $[Eu_2(Mell)(H_2O)_8]$ was modified with the purpose of producing large crystals and to obtain phase-pure MOFs with Tb^{3+} and Gd^{3+} ions. In an optimized synthetic approach, undisturbed solutions containing stoichiometric ratio 1:1 (metal:ligand) produced well-developed crystals with dimensions varying from 1.39-1.95 x 1.39-1.91 x 0.62-1.90 mm. Detailed synthetic approaches are described at the Support Information. A representation of the steps to obtain layer-by-layer white-light emitting Ln-MOF material and *R-MOF*, *B-MOF* and *G-MOF* crystals under UV excitation are displayed in Scheme 1. The excitation, emission spectra and lifetime decay curves of *R-MOF*, *B-MOF*

and *G-MOF* are displayed in Figure 2S in Supporting information. In Figure 2 are exposed the emission spectra and CIE diagram for a sample designed as MixLn-MOF, which is composed by a randomized distribution of Eu^{3+}, Tb^{3+}, Gd^{3+} ions (1:1:1) in the ($[Ln_2(Mell)(H_2O)_8]$ matrix. Fundamentally, this experiment proves that the usual strategy adopted to produce white-light emitting materials, is considerably affected by energy transfer (ET) due to the random distribution of the color centers. The emission spectra profiles of MixLn-MOF show a predominance of the Eu^{3+} emission (red color) in detriment of the ligand (blue color) and Tb^{3+} (green color) emissions, result in a limited production of color tones.

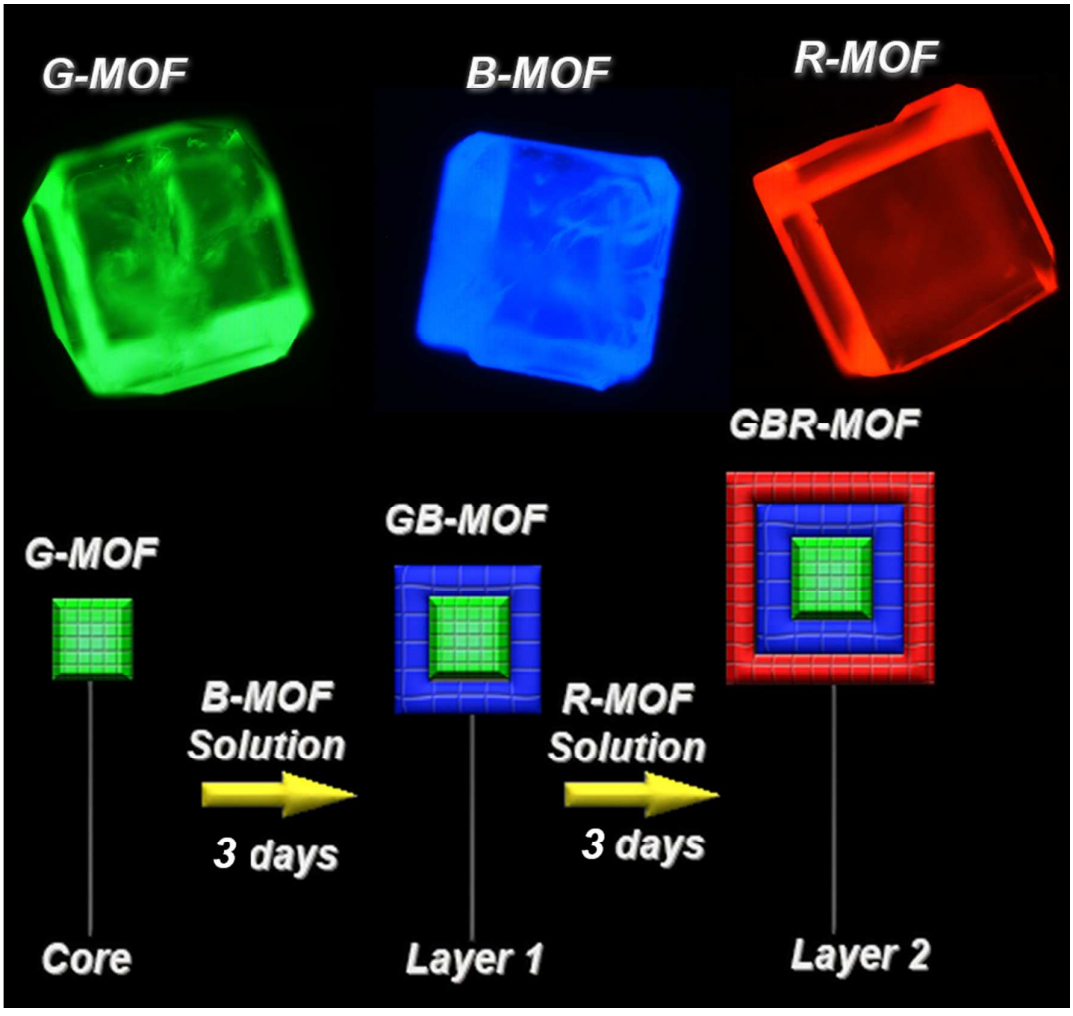

Figure 1. Optical microscopy of *R-MOF*, *B-MOF* and *G-MOF* under UV excitation. Illustration of the strategy to produce layer-by layer white-light emitting Ln-MOF material.

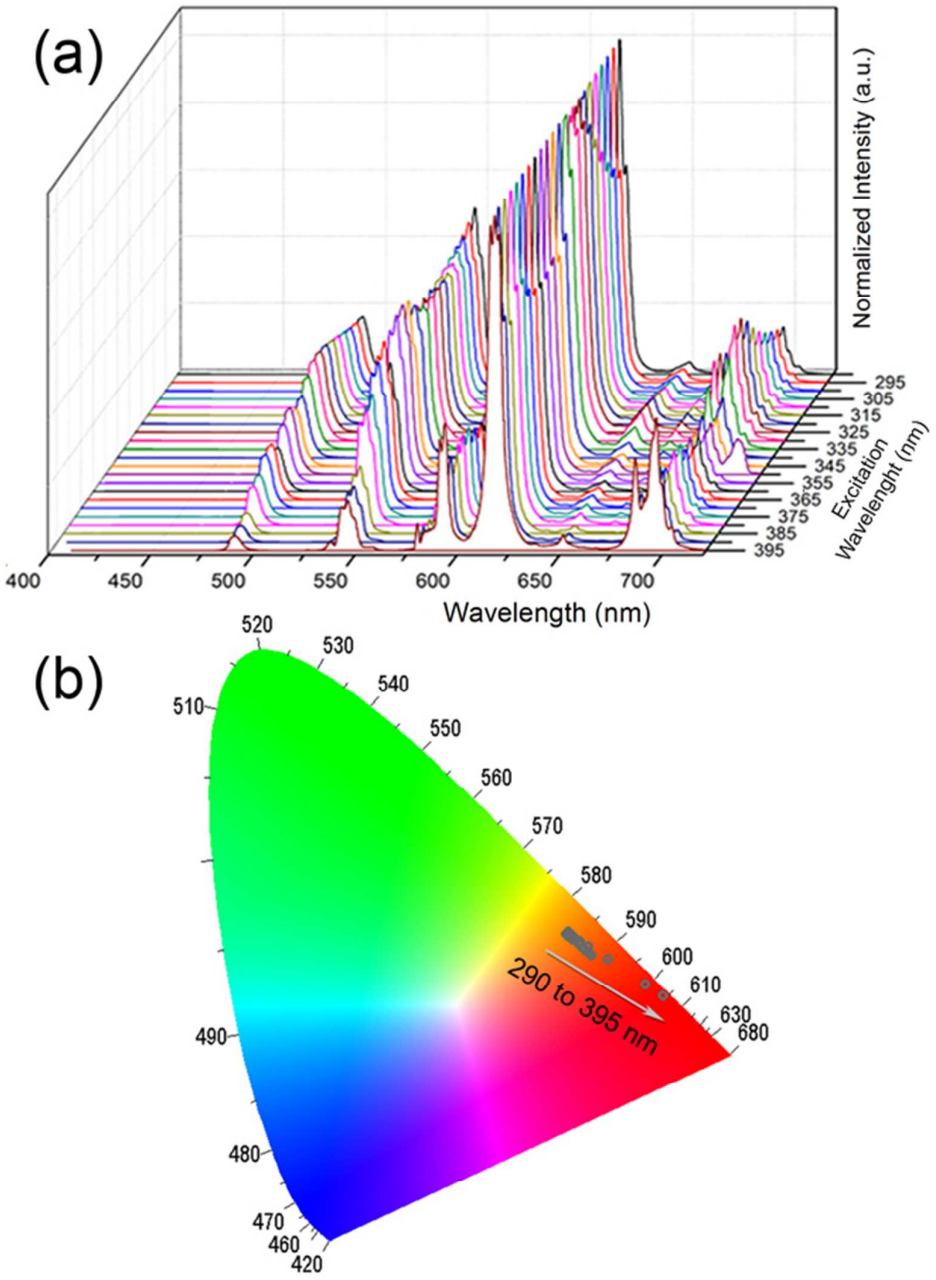

Figure 2. (a) Emission spectra of MixLn-MOF. (b) CIE chromatic diagram.

Previous reports have showed that the ET modulation among color centers in system randomly arranged is not a simple task.[17] The decay curves of Tb^{3+} and Eu^{3+} have presented a non-exponential components, indicating distinct interaction levels between the subpopulation of the Tb^{3+} and Eu^{3+} ions. Although these ones find themselves in the same crystal domain, the slow Tb^{3+}—Tb^{3+} energy migration induces a non-exponential behavior, at short time

domains, due to the direct ET to the nearest Eu^{3+} ion. On the other hand, at long time domains the decay curve displays an exponential component, caused by the energy diffusion among the Tb^{3+} ions. The lifetime values for Eu^{3+} and Tb^{3+}, acquired at room temperature upon excitation at 374 nm are 0.14 and 0.30, and 0.22 and 0.51 ms, respectively. The ligand-to-metal ET has been estimated in order of 10^6 to10^9 s^{-1}. If the effect of the lanthanide contraction has not been considered, the ET rate (k_{ET}), efficiency (η_{ET}) and the critical transfer distance of the $Tb^{3+}\rightarrow Eu^{3+}$ process were estimated by Equation (1)-(3)[16, 28]

$$k_{ET} = \tau_1^{-1} - \tau_0^{-1} \quad \textbf{(1)}$$

$$\eta_{ET} = \frac{\tau_1^{-1} - \tau_1^{-1}}{\tau_1^{-1}} \quad \textbf{(2)}$$

$$k_{ET} = \tau_0^{-1}\left(\frac{R_0}{R}\right)^S \quad \textbf{(3)}$$

where R is the Ln^{3+} ions pair distance (6.11 Å), R_0 is the critical transfer distance and S= 6, 8, 10 for *dipole—dipole*, *dipole—quadrupole* and *quadrupole—quadrupole* interactions, respectively. While τ_0 and τ_1 are florescence lifetimes monitoring $^5D_4$ emission of Tb^{3+} ion at 545 nm of *G-MOF* and MixLn-MOF. In the MixLn-MOF the blue emission is fully quenched, while the intensity of $^5D_4\rightarrow{}^7F_5$ transition of Tb^{3+} ion is reduced by 40% in comparison with *G-MOF* (see Supporting Information). This is justified by a $Tb^{3+}\rightarrow Eu^{3+}$ ET rate (k_{ET}) of 2878.8 s^{-1} and η_{ET} of 63.3%, considering that the ET mechanism is governed by dipole electric-dipole electric interaction.[16, 29, 30] The R_0 value of 6.70 Å enables the Tb^{3+} ion to transfer energy efficiently to Eu^{3+} ions, which can occupy the sites at 6.11 and 6.62 Å. These results indicate that only Eu^{3+} ions in ideal distance can be apt to be excited by Tb^{3+} ions, whereas those outside this criterion are exclusively excited via ligands or $Eu^{3+}\rightarrow Eu^{3+}$ energy migration. This hypothesis is supported by the non-exponential decay emission from the Eu^{3+} cation in the MixLn-MOF.

As discussed above, although the construction of white-light emitters may be obtained

via an additive color mixing approaches (red, green and blue-emitters), the ET plays a limiting role on the ability to tune systematically the emissions from specific emitter centers inserted in the same host domain. In terms of epitaxy, it can be performed by rigorous growth control of the R, G and B emissive layers. In Figure 3 shows the emission spectra of the four models of different multiemitter layer-by-layer architectures.

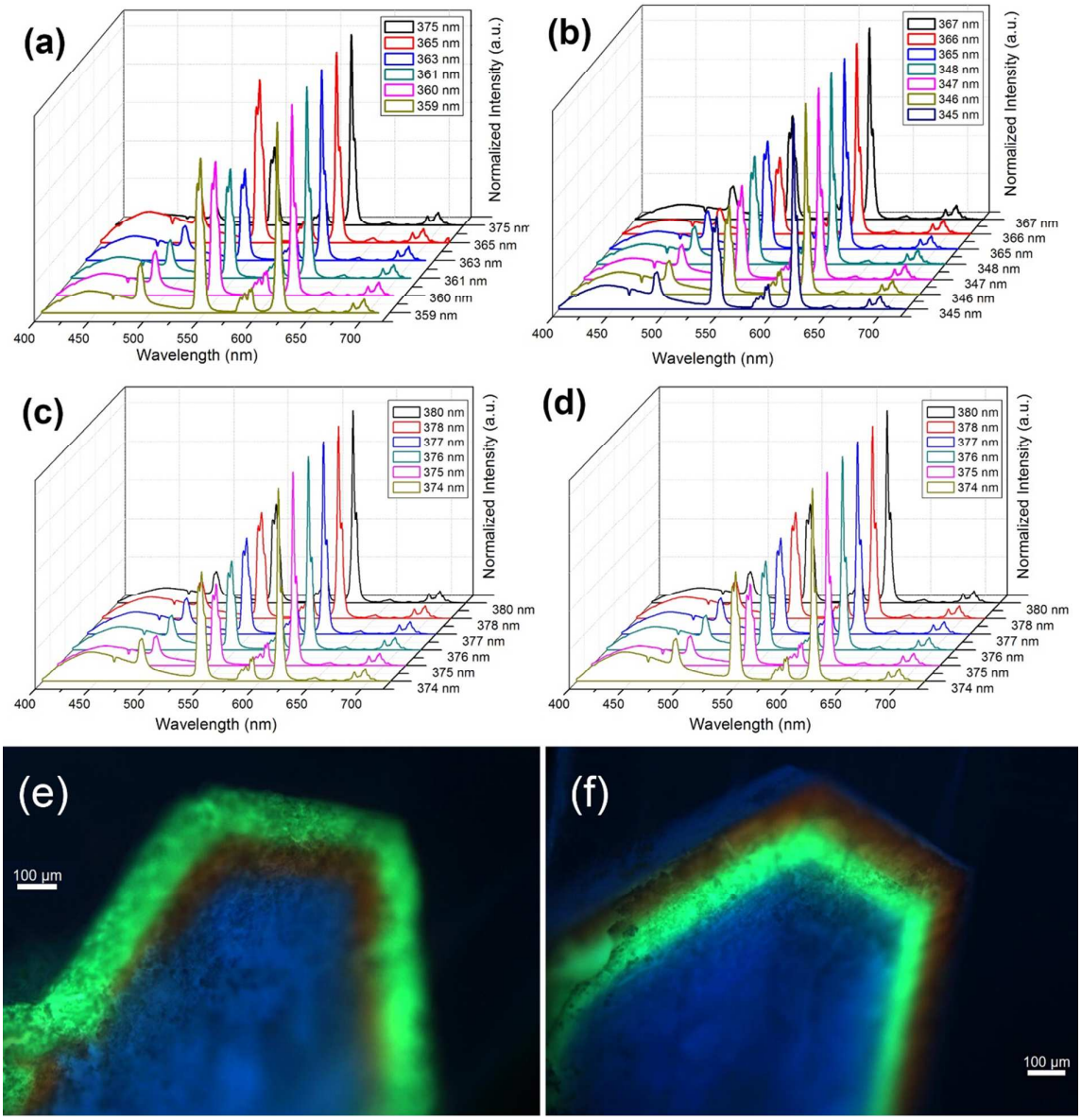

Figure 3. Emission spectra acquired at room temperature of multiemitter layer-by-layer Ln-MOF. (a): *RGB-MOF*; (b): *RBG-MOF*; (c): *BRG-MOF*; (d): *BGR*; (e) and (f): Images of fluorescence microscopy obtained upon excitation at 256 nm for *BRG-MOF* and *BGR-MOF*, respectively. Bar scale of 100 µm.

The photoluminescence emission spectra of the *RGB, RBG, BRG* and *BGR* materials acquired at room temperature upon excitation at UV region (see the insets in Figure 3) have presented bands centered at 440, 545 and 617 nm, which were provided by the blue, green and red emissions of the organic ligand, Tb^{3+} and Eu^{3+} ions, respectively. The emission spectra have demonstrated sensible dependence of excitation wavelength, since the relative amplitude of the emission transitions have presented substantial alterations upon distinct excitations. The emission spectra exhibited in Figure 3 arose from the optimized excitation wavelengths for production of the white light. As shown in Figure 3 (e) and (f), the emission microscopy images reveal core-shell crystals with color emission contrasts corresponding to *R*-, *G*- and *B-MOF*.

In order to investigate the energy transfer among R, G and B layers, lifetime curves of *BGR-MOF* and *BRG-MOF* were acquired at room temperature by monitoring of the maxima emission at 615 nm upon excitation at 395 nm, 545 and 615 nm upon excitation at 378 nm, and 440, 545 (BGR-MOF) and 615 nm (BRG-MOF) upon excitation at 336 nm. Decay curves (Figures 14S and 15S) display predominantly monoexponential profile and lifetime of 0.18 - 0.21 ms (0.20 ms for *R-MOF* material), 0.59 – 0.61ms (0.60 ms for *G-MOF*) and 3.98 – 4.0 ms (3.35 ms for *B-MOF*). The biexponencial profile presented by *BRG-MOF*, through monitoring of the maxima emission at 615 nm upon excitation at 336 are assigned to $^5D_0 \rightarrow {}^7F_2$ transition of Tb^{3+} ion and $^5D_4 \rightarrow {}^7F_3$ transition of Eu^{3+} ion in the layer one and layer two, respectively. It is important to note that although the pictures displayed in Figure 3 (e) and (f) have presented transmetalations regions, the lifetimes values are important evidence that the energy transfer among the different layers plays a secondary role in the different multiemitter layer-by-layer architectures material. These results confirm the hypothesis that to segregate of color emitter centers via epitaxially grown layers preserves intact the optical

properties of the respective pure materials. Figure 4 illustrates the CIE chromaticity diagrams[31] and CIE coordinates values of *RGB-MOF*, *RBG-MOF*, *BRG-MOF* and *BGR*.

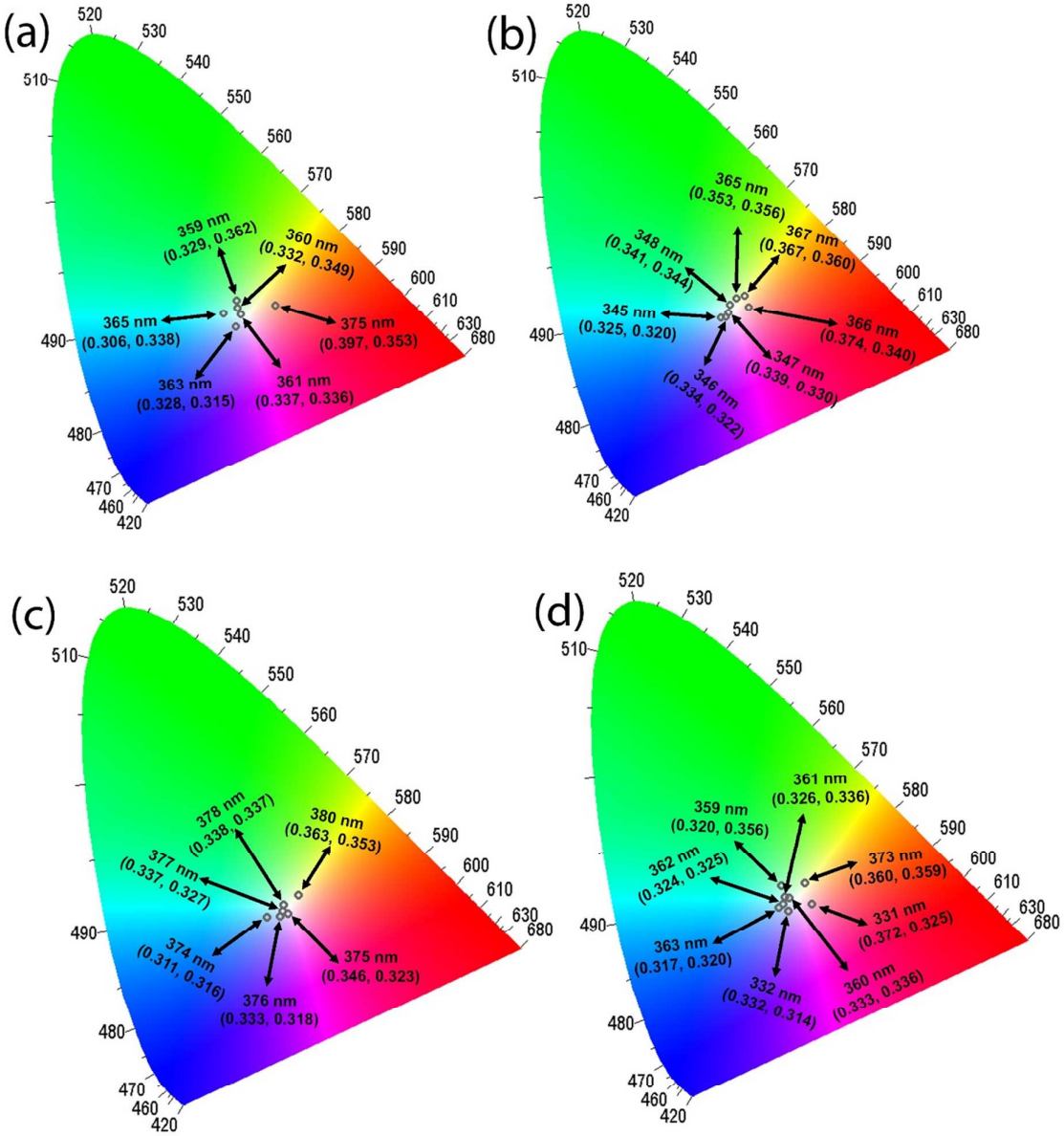

Figure 4. CIE chromaticity diagrams and CIE coordinate values (x,y). (a): *RGB*; (b): *RBG*; (c): *BRG*; (d): *BGR*.

The CIE has established that the ideal white light may be reached by optimized mixing emission of R, G and B emitters with following coordinates (0.33, 0.33).[6] The CIE diagrams show several points close which fall close to the white region by fine tune of the excitation

wavelength. The white-light emission were obtained with CIE coordinates of (0.337, 0.336), (0.339, 0.330), (0.338, 0.337) and (0.333, 0.336) for *RGB-MOF*, *RBG-MOF*, *BRG-MOF* and *BGR,* respectively. In summary, we have successfully produced four multiemitter Ln-MOF materials by enable the design of white-light emitting materials. The energy transfer among the emitter centers were controlled by constraining them in specific regions of the crystal domain. This strategy that each emitter layer actuate like an independent crystals, keeping the integrity of its optical properties

SUPPORTING INFORMATION

The experimental procedure, crystal strucuture, x-ray powder patterns, spectroscopic data of the materials. This material is available free of charge via internet at http://pubs.rsc.org.

AUTHOR INFORMATION

Corresponding author footnote.

* Prof. Dr. Marcelo O. Rodrigues (*marcelozohio@unb.br*), *LIMA-Laboratório de Inorgânica e Materiais, Campus Universitário Darcy Ribeiro, CEP 70904970, P.O.Box 4478, Brasilia-DF, Brazil.* Fax: (+) 55 (61) 32734149; Phone (+)55 (61) 31073867

* Prof. Dr. Severino Alves Júnior (*salvesjr@ufpe.br*) *Departamento de Química Fundamental*, UFPE, 50670-901, Recife, PE, Brazil. Tel. (+) 55 (81) 2126-7475; Fax: (+) 55 (81) 2126-8442;

AKNOWLEDGEMENT

The authors gratefully acknowledge CNPq (INCT/INAMI and RH-INCT/INAMI), DPP-UNB. FAP-DF (Edital-5/2013), FACEPE (APT-0859—1.06/08), FAPITEC/SE and CAPES for its financial support.

REFERENCES

1. S. Choi, Y. J. Yun and H.-K. Jung, *Mater. Lett.*, 2012, **75**, 186-188.

2. A. C. Grimsdale, K. Leok Chan, R. E. Martin, P. G. Jokisz and A. B. Holmes, *Chem. Rev.*, 2009, **109**, 897-1091.

3. P. O. Anikeeva, J. E. Halpert, M. G. Bawendi and V. Bulović, *Nano Lett.*, 2009, **9**, 2532-2536.

4. Z. Yu, X. Niu, Z. Liu and Q. Pei, *Adv. Mater.*, 2011, **23**, 3989-3994.

5. Z. Lin, Y.-D. Lin, C.-Y. Wu, P.-T. Chow, C.-H. Sun and T. J. Chow, *Macromolecules*, 2010, **43**, 5925-5931.

6. D. F. Sava, L. E. S. Rohwer, M. A. Rodriguez and T. M. Nenoff, *J. Am. Chem. Soc.*, 2012, **134**, 3983-3986.

7. M. D. Allendorf, C. A. Bauer, R. K. Bhakta and R. J. T. Houk, *Chem. Soc. Rev.*, 2009, **38**, 1330-1352.

8. Y. Cui, Y. Yue, G. Qian and B. Chen, *Chem. Rev.*, 2012, **112**, 1126-1162.

9. C. Wang, T. Zhang and W. Lin, *Chem. Rev.*, 2011, **112**, 1084-1104.

10. M. O. Rodrigues, F. A. Paz, R. O. Freire, G. F. de Sá, A. Galembeck, M. C. Montenegro, A. N. Araújo and S. Alves, *J. Phys. Chem. B*, 2009, **113**, 12181-12188.

11. A. Cadiau, C. D. S. Brites, P. M. F. J. Costa, R. A. S. Ferreira, J. Rocha and L. D. Carlos, *ACS Nano*, 2013, **7**, 7213-7218.

12. X. Rao, T. Song, J. Gao, Y. Cui, Y. Yang, C. Wu, B. Chen and G. Qian, *J. Am. Chem. Soc.*, 2013, **135**, 15559-15564.

13. I. T. Weber, A. J. Geber de Melo, M. A. de Melo Lucena, M. O. Rodrigues and S. Alves Junior, *Anal. Chem.*, 2011, **83**, 4720-4723.

14. I. T. Weber, I. A. A. Terra, A. J. G. d. Melo, M. A. d. M. Lucena, K. A. Wanderley, C. O. Paiva-Santos, S. G. Antonio, L. A. O. Nunes, F. A. A. Paz, G. F. d. Sá, S. A. Júnior and M. O. Rodrigues, *RSC Adv.*, 2012, **2**, 3083-3087.

15. Y. Cui, W. Zou, R. Song, J. Yu, W. Zhang, Y. Yang and G. Qian, *Chem. Commun.*, 2014, **50**, 719-721.

16. J. He, M. Zeller, A. D. Hunter and Z. Xu, *J. Am. Chem. Soc.*, 2011, **134**, 1553-1559.

17. N. Kerbellec, D. Kustaryono, V. Haquin, M. Etienne, C. Daiguebonne and O. Guillou, *Inorg. Chem.*, 2009, **48**, 2837-2843.

18. Y.-H. Zhang, X. Li and S. Song, *Chem. Commun.*, 2013, **49**, 10397-10399.

19. Q. Tang, S. Liu, Y. Liu, D. He, J. Miao, X. Wang, Y. Ji and Z. Zheng, *Inorg. Chem.*, 2013, **53**, 289-293.

20. Y. Luo, G. Calvez, S. Freslon, K. Bernot, C. Daiguebonne and O. Guillou, *Eur. J. Inorg. Chem.*, 2011, **2011**, 3705-3716.

21. Z. Wang, Y. Yang, Y. Cui, Z. Wang and G. Qian, *J. Alloys Compd.*, 2012, **510**, L5-L8.

22. M. O. Rodrigues, J. D. L. Dutra, L. A. O. Nunes, G. F. de Sá, W. M. de Azevedo, P. Silva, F. A. A. Paz, R. O. Freire and S. A. Júnior, *J. Phys. Chem. C*, 2012, **116**, 19951-19957.

23. M. L. Foo, R. Matsuda and S. Kitagawa, *Chem. Mater.*, 2013, **26**, 310-322.

24. K. Koh, A. G. Wong-Foy and A. J. Matzger, *Chem. Commun.*, 2009, 6162-6164.

25. S. Furukawa, K. Hirai, Y. Takashima, K. Nakagawa, M. Kondo, T. Tsuruoka, O. Sakata and S. Kitagawa, *Chem. Commun.*, 2009, 5097-5099.

26. B. Liu, M. Ma, D. Zacher, A. Bétard, K. Yusenko, N. Metzler-Nolte, C. Wöll and R. A. Fischer, *J. Am. Chem. Soc.*, 2011, **133**, 1734-1737.

27. W. Liang Ping, M. Munakata, T. Kuroda-Sowa, M. Maekawa and Y. Suenaga, *Inorg. Chim. Acta*, 1996, **249**, 183-189.

28. Y.-P. Sun, B. Zhou, Y. Lin, W. Wang, K. A. S. Fernando, P. Pathak, M. J. Meziani, B. A. Harruff, X. Wang, H. Wang, P. G. Luo, H. Yang, M. E. Kose, B. Chen, L. M. Veca and S.-Y. Xie, *J. Am. Chem. Soc.*, 2006, **128**, 7756-7757.

29. J. Zhou, C. Booker, R. Li, X. Zhou, T.-K. Sham, X. Sun and Z. Ding, *J. Am. Chem. Soc.*, 2007, **129**, 744-745.

30. A. R. Ramya, D. Sharma, S. Natarajan and M. L. P. Reddy, *Inorg. Chem.*, 2012, **51**, 8818-8826.

31. F. S. T. P.A. Santa-Cruz, *Spectra Lux Software v.2.0, Ponto Quântico Nanodispositivos, UFPE*, 2003.